

## Interface Debonding and Fiber Cracking in Brittle Matrix Composites

Anthony G. Evans\* and Ming Y. He

Materials Department, College of Engineering, University of California,  
 Santa Barbara, California 93106

John W. Hutchinson\*

Applied Sciences Division, Harvard University, Cambridge, Massachusetts 02138

Analyses of debonding along interfaces and of the kinking of interface cracks into a fiber have been used to define the role of debonding in fiber-reinforced, brittle matrix composites. The results reveal that, for fibers *aligned* with the tensile stress axis, debonding requires an interface fracture energy,  $\Gamma_i$ , less than about one-fourth that for the fiber,  $\Gamma_f$ . Furthermore, once this condition is satisfied, it is shown that fiber failure does not normally occur by deflection of the debond through the fiber. Instead, fiber failure is governed by weakest-link statistics. The debonding of fibers *inclined* to the stress axis occurs more readily, such that debonds at acutely inclined fibers can deflect into the fiber, whereupon the failure of fibers is dominated by their toughness. [Key words: composites, mechanical properties, cracks, interfaces, fibers.]

### I. Introduction

**B**RITTLE matrices reinforced with brittle fibers may exhibit high "toughness" when fiber failure is suppressed at the matrix crack front.<sup>1-5</sup> This process involves interface debonding at the crack front and probably further debonding in the crack wake,

Y. S. Kim—contributing editor

Manuscript No. 198706. Received January 3, 1989; approved May 1, 1989.  
 \*Member, American Ceramic Society.

accompanied by frictional sliding along the debonded interfaces (Fig. 1). Fiber failure in the crack wake results in a pullout contribution to toughness, which becomes large when the distance between the fiber failure site and the matrix crack plane (i.e., the pullout length) is also large. Consequently, it is important to understand the mode of fiber failure and the relationships which govern the fiber failure site. Existing analyses of pullout toughening have assumed that fiber failure involves weakest-link statistics,<sup>6</sup> whereupon the failure site depends on fiber strength parameters. Such solutions have dictated present approaches for fiber development which emphasize *strength*. However, implicit in these analyses is the premise that fiber failure does not occur by kinking from the debond crack tip into the fiber. Clearly, should fiber failure instead proceed by kinking, the relevant fiber property would be its *toughness* rather than its strength, resulting in very different emphasis for fiber development. The existence of a kinking mechanism of fiber failure has been illustrated in SiC-whisker-reinforced  $\text{Al}_2\text{O}_3$ <sup>7,8</sup> (Fig. 2), at whiskers acutely inclined to the matrix crack plane.

The intent of the present article is to utilize some basic mechanics<sup>9,10</sup> to address both initial debonding and fiber failure by kinking. For this purpose, two important parameters used throughout the paper are now introduced. The first is the Dundurs parameter  $\alpha$ , which is a measure of the elastic mismatch between the fiber and matrix:<sup>11</sup>

$$\alpha = (\bar{E}_f - \bar{E}_m) / (\bar{E}_f + \bar{E}_m) \quad (1)$$

with  $\bar{E}$  being the plane strain tensile modulus and the subscripts *f* and *m* referring to the fiber and matrix, respectively. The second

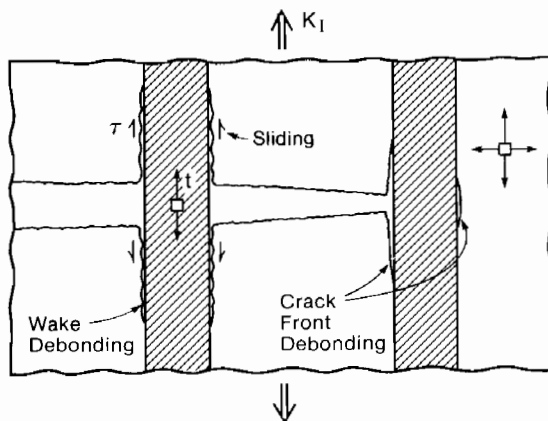


Fig. 1. Schematic indicating the debonding and sliding behaviors that accompany matrix crack propagation in a brittle matrix composite: *t* is the axial stress on the fibers between the crack surfaces and  $\tau$  is the sliding stress along the debonded interfaces.

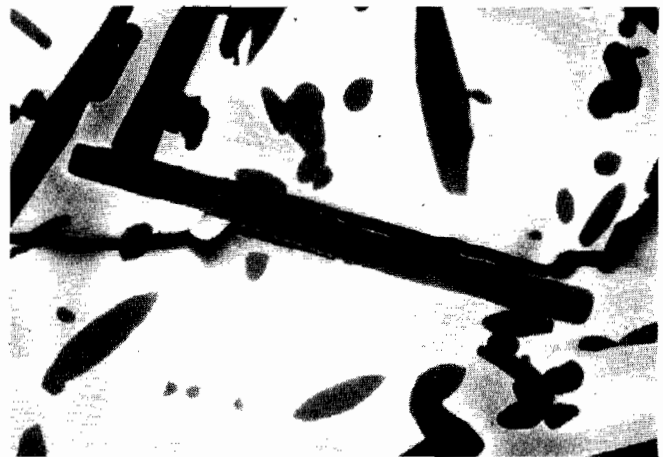


Fig. 2. Debonding of an inclined SiC whisker in an  $\text{Al}_2\text{O}_3$  matrix. A thin ( $\sim 5$  nm) amorphous silicate layer at the interface allows debonding.<sup>7,8</sup> Also note that a whisker crack has formed from the end of one of the debonds.

parameter is the phase angle of loading,  $\psi_i$ , associated with debonds given by<sup>8,9</sup>

$$\psi_i = \tan^{-1}(k_2/k_1) \quad (2)$$

where  $k_2$  and  $k_1$  are the imaginary and real components of the stress intensity factor at the debond. In essence,  $\psi_i$  is a measure of the mode mixity of the debond crack, such that  $\psi_i = 0$  refers to pure opening and  $\psi_i = \pi/2$  represents pure shear.

II. Basic Mechanics

The incidence of *initial debonding* at the matrix crack front can be assessed from a comparison of two values of the strain energy release rate,  $\mathcal{G}$ : the plane strain value  $\mathcal{G}_i$  for a *small* interface kink which emanates from the matrix crack, compared with the value  $\mathcal{G}_f$  for a small coplanar kink into the fiber<sup>6</sup> (Fig. 3). Specifically, debonding is expected to occur when  $\mathcal{G}_i/\mathcal{G}_f$  is larger than the ratio of fracture energies,  $\Gamma_i/\Gamma_f$ , at the relevant phase angle of loading for the interface crack,  $\psi_i$ . The solution of this problem depends somewhat on the mode of loading experienced by the matrix crack. For maximum relevance, all solutions presented in this paper refer to a matrix crack subject to mode I loading.

For brittle matrix composites containing fibers *aligned* with the tensile stress axis, the debonding diagram for a matrix crack nor-

\*Delamination by matrix crack propagation parallel to the fibers can also occur; this problem is not addressed by the present study.  
 †The maximum  $\mathcal{G}$ , taken with respect to the kink angle, is presumed to govern the incidence of fiber cracking. The result is independent of debond length and kink length because the kink can be infinitesimally small compared with the debond.

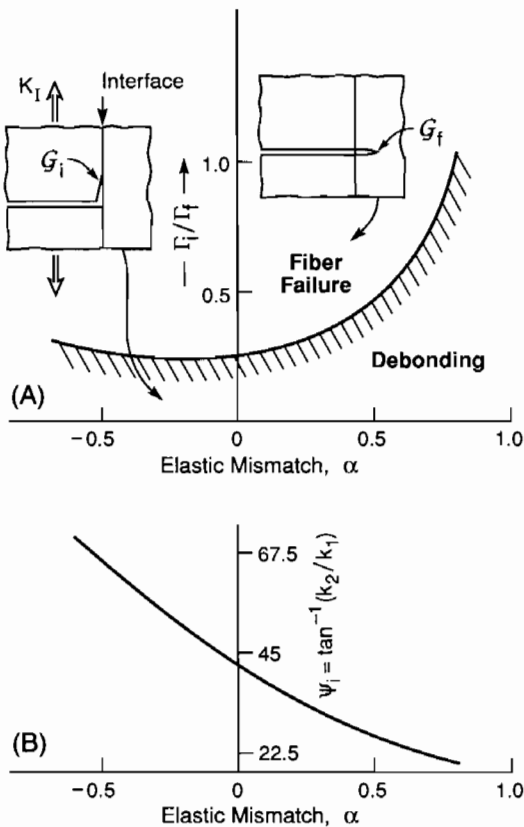


Fig. 3. (A) Crack front debond diagram indicating the range of relative interface fracture energy,  $\Gamma_i/\Gamma_f$ , in which debonding occurs in preference to fiber failure:  $\alpha$  is a measure of the elastic mismatch<sup>11</sup> ( $\alpha = (\bar{E}_f - \bar{E}_m)/(\bar{E}_f + \bar{E}_m)$ , where  $\bar{E} = E/(1 - \nu^2)$  is the plane strain tensile modulus: positive  $\alpha$  refers to a fiber having higher modulus than the matrix). (B) Trends in phase angle at the debond crack with  $\alpha$ :  $k_2$  and  $k_1$  are defined in Eq. (2).

mal to the interface (Fig. 3)\* indicates that the condition  $\Gamma_i/\Gamma_f < 1/4$  always permits debonding, albeit that debonding occurs more readily for *higher-modulus* fibers. Furthermore, because only small kinks need be considered, the result is applicable to both fibers and laminates, in plane strain, as well as being unaffected by the residual strain. In a composite containing *inclined* fibers,  $\mathcal{G}_i/\mathcal{G}_f$  increases as the interface angle  $\phi$  decreases and, consequently, debonding occurs subject to less stringent requirements on  $\Gamma_i/\Gamma_f$  (Fig. 4).

When the condition for initial debonding represented by Figs. 3 and 4 is satisfied, it is immediately evident that the crack can deviate from the interface into the fiber only if the phase angle of loading at the debond changes and/or  $\Gamma_i/\Gamma_f$  increases. Appreciable changes in the phase angle at the debond become possible as an intact fiber enters the *crack wake*, because of changes in loading on the fiber,<sup>12</sup> coupled with residual strain effects. Good insight into these effects can be gained by examining the behavior of a fiber in the immediate crack wake (Fig. 5). Specifically, the phase angle changes rapidly as axial loads are exerted on the fiber between the crack surfaces, even without further debonding (Fig. 5(A)), especially when residual strain exists,<sup>12</sup> as characterized by a misfit strain,  $\epsilon$ . Furthermore, the phase angle for the debond may increase as the debond extends (Fig. 5(B)). This change in phase angle between the crack front and the crack wake could, in principle, cause fiber failure from the debond.

The problem of *fiber failure* involves a comparison of the *maximum* value of the strain energy release rate for a small kink into the fiber, with the strain energy release rate for a similarly small kink continuing along the interface<sup>10</sup> (Fig. 6).† Calculations of these energy release rates in plane strain compared with critical values for the fiber  $\Gamma_f$  and interface  $\Gamma_i$  provide the fiber failure diagram indicated in Fig. 6. In this diagram, the *loci of initial debonding*, plotted for fibers inclined at  $\phi = \pi/2$  and  $\phi = \pi/3$  (Fig. 4), refer to debond requirements ascertained from Fig. 3, but now with  $\Gamma_i/\Gamma_f$  plotted against  $\phi_i$  such that *each point refers to a specific*  $\alpha$ . Three such  $\alpha$  values are indicated in the figure. It is vividly apparent that, for  $\phi = \pi/2$ , fiber failure typically requires larger values of  $\Gamma_i/\Gamma_f$  than that needed for initial debonding. Consequently, if the ratio  $\Gamma_i/\Gamma_f$  is fixed and thus independent of the phase angle,  $\psi_i$ , a debond, once initiated, would *always remain at the interface*. A similar conclusion has been reached for the delamination problem.<sup>13</sup> Possible changes in this conclusion, based on phase angle effects, are discussed below. Equivalent analysis for *inclined fibers* indicates that the energy release rate for kinking into the fiber can become smaller than that for

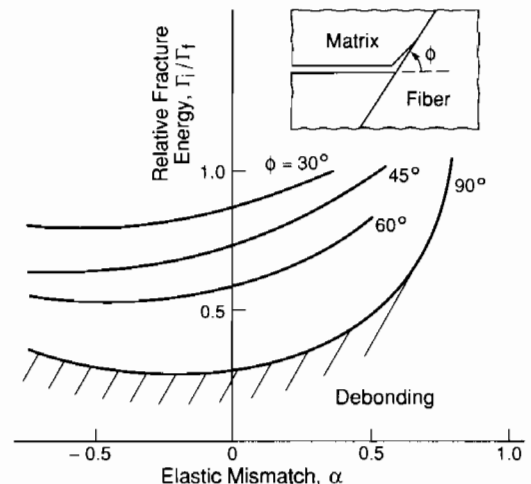


Fig. 4. Effect of interface orientation on the debonding requirements.

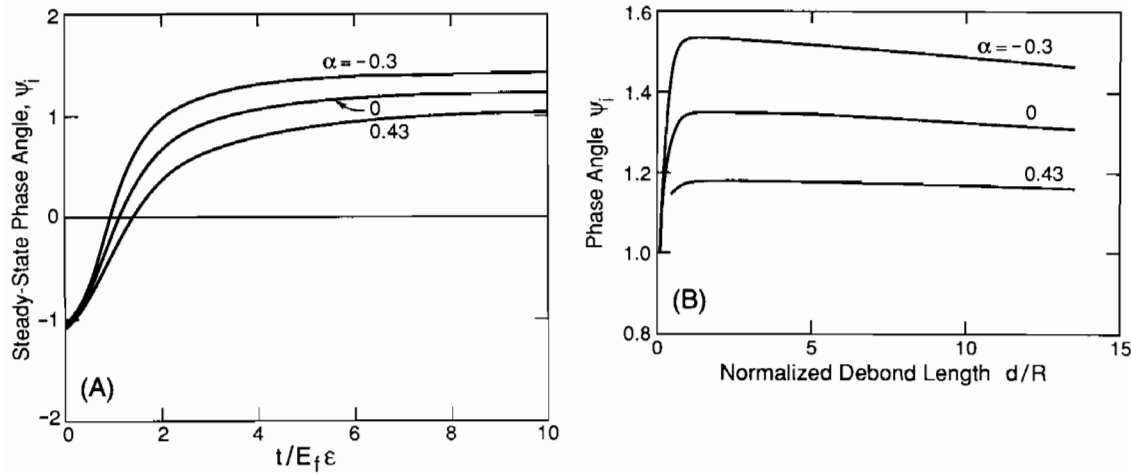


Fig. 5. Trends in phase angle at the debond,  $\psi_i$ , for a fiber loaded in the crack wake: (A) effect of positive mismatch strain  $\epsilon$  (interface tension) in the steady-state region ( $\psi_i$  independent of  $d$ ). (B) effect of debond length  $d$  when mismatch strain  $\epsilon$  is zero; note that  $\psi_i$  for large  $t/E_f \epsilon$  in Fig. 5(A) coincides with the steady-state values, as required.

initial debonding when  $\phi \leq \pi/3$ . Consequently, fibers having inclinations in this range can fail by kinking, even when  $\Gamma_i$  is independent of  $\psi_i$ . A change in fiber failure mode thus becomes possible at fiber inclination  $\phi \approx \pi/3$ .

The interface fracture energy,  $\Gamma_i$ , is often influenced by the

<sup>†</sup>Consistent with the condition that crack propagation in homogeneous brittle solids seeks the trajectory having zero phase angle.<sup>15</sup>

phase angle,  $\psi_i$ .<sup>14</sup> The role of the phase angle is not fully understood. One hypothesis is that crack surface contact at asperities on the interface crack surface becomes increasingly important as  $\psi_i$  increases, causing a corresponding increase in  $\Gamma_i$  (Fig. 7). Alternative mechanisms that could cause  $\Gamma_i$  to increase with  $\psi_i$  have yet to be explored. The fracture resistance of a homogeneous fiber  $\Gamma_f$  does not involve similar considerations, because the maximum energy release rate essentially coincides with the orientation at which the phase angle in the fiber  $\psi_f \approx 0$ .<sup>4</sup> However, fracture energy anisotropy in the fibers would introduce a variant that requires further investigation.

### III. Debonding and Fiber Failure

The prerequisite for good composite performance is that crack front debonding occurs, as governed by the fracture resistance ra-

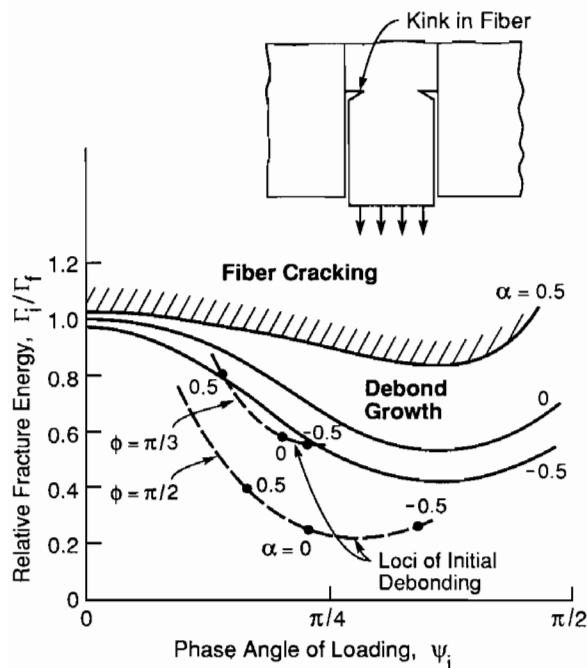


Fig. 6. Fiber cracking diagram for a fiber loaded in the crack wake. In this diagram, the solid lines demarcate the boundaries between fiber cracking (above the line) and debond growth (below the line). Each line refers to a specific value of  $\alpha$ . Also shown is the locus for crack front debonding, over the same range of  $\alpha$ . This locus is the debond boundary in  $\Gamma_i/\Gamma_f$ ,  $\psi_i$  space, with each point on the boundary referring to a specific  $\alpha$ : for reference purposes, three typical values of  $\alpha$  are shown. This figure indicates the extent to which  $\Gamma_i/\Gamma_f$  must increase between the crack front and the wake in order to have debond deflection into the fiber.

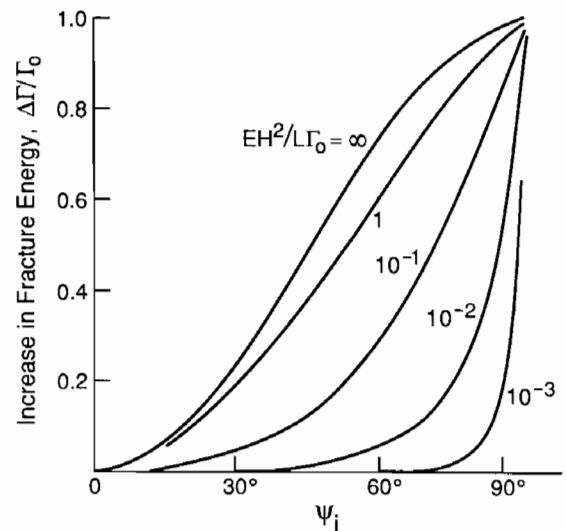


Fig. 7. Some trends in critical energy release rate for interface cracking,  $\Gamma_i$ , with the phase angle of loading,  $\psi_i$ , predicted for a rough interface, with  $H$  being the amplitude,  $L$  the wavelength of the roughness, and  $E$  Young's modulus.  $\Delta\Gamma = \Gamma_i - \Gamma_0$  is the increase in fracture energy over the value  $\Gamma_0$  which obtains at  $\psi_i = 0$ .

tio,  $\Gamma_i/\Gamma_f$  (Figs. 3 and 4). However, the tendency for further debonding in the wake depends on additional variables. The basic characteristics are summarized in composite diagrams (Fig. 8). As already noted, such diagrams reveal that, when  $\Gamma_i$  is independent of the phase angle,  $\psi_i$ , fiber failure can occur from the end of the debond *only* if the fiber axis has an inclination with the matrix crack plane in the range  $\phi \approx \pi/3$ . Even then, the phase angle must increase to cause  $\Gamma_i/\Gamma_f$  to intersect the fiber failure boundary (Fig. 8). However, such changes in phase angle become possible as the fiber enters the crack wake, as illustrated by comparing Figs. 3 and 5. The crack/fiber interactions depicted in Fig. 2 exemplify such a case. For this material ( $\text{Al}_2\text{O}_3/\text{SiC}$ ), debonding conditions at the crack front governed by  $\Gamma_i/\Gamma_f$  are marginally satisfied for those fibers having inclination  $\phi \approx \pi/3$ . Consequently, such fibers subsequently fail by kinking from the debond.

The interpretation of fiber failure using composite diagrams and based on the notion that  $\Gamma_i$  be independent of  $\psi_i$  is conservative, because of possible changes in  $\Gamma_i$  with  $\psi_i$  (Fig. 7). Some relevant issues are illustrated in Fig. 8 for the case  $\phi \approx \pi/2$  and  $\alpha = 0$ . For this case, at the crack front  $\psi_i \approx \pi/4$  (Fig. 3(B)), whereas as the fiber becomes stressed in the crack wake, a maximum in  $\psi_i$  between  $5\pi/6$  and  $\pi/2$  is reached, dependent upon the residual strain (Fig. 5(B)). The change in  $\Gamma_i$  within the range of phase angles between  $\pi/4$  and  $\pi/2$  is thus of relevance. It is qualitatively apparent that  $\Gamma_i$  can increase sufficiently to cause  $\Gamma_i/\Gamma_f$  to enter the fiber failure zone within this range of phase angles. However, it is also apparent that the change in  $\Gamma_i$  associated with roughness (Fig. 7) would generally be insufficient for this purpose. Further understanding of changes in  $\Gamma_i$  with  $\psi_i$  is needed to provide additional insight.

#### IV. Concluding Remarks

The preceding discussion suggests that in composites with fibers aligned along the stress axis, interface debonding should occur, provided that the fracture resistance of the "weakest" interface (matrix/coating or coating/fiber) satisfies the inequality,  $\Gamma_i/\Gamma_f \leq 1/4$ . When this condition is satisfied, further debonding occurs in the crack wake in preference to fiber failure from the debond, unless an interface mechanism exists that causes  $\Gamma_i$  to increase rapidly with increase in phase angle,  $\psi_i$ . Consequently, the influence of the mechanical properties of the *fiber* on composite behavior is contained exclusively in the statistical parameters that govern their tensile strength.<sup>6</sup>

In composites with randomly oriented fibers, debonding occurs more readily at the more acutely inclined reinforcements. Then, in cases wherein debonding is marginal and occurs only at the inclined reinforcements, fiber failure by kink fracture from the debond is feasible. For such materials, fiber *toughness* rather than fiber strength is the fiber property that governs the composite toughness.<sup>7,8</sup>

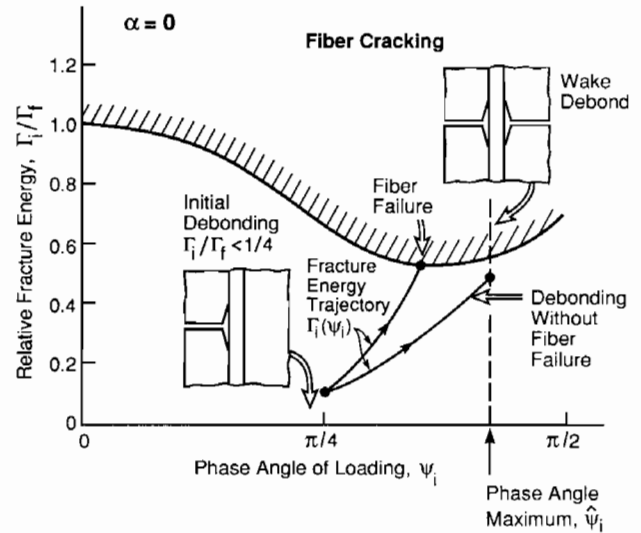


Fig. 8. Composite diagram concerning fiber failure plotted for materials having  $\alpha = 0$ . Trajectories of  $\Gamma_i$  with  $\psi_i$  that cause either debond deflection into the fiber or debonding without fiber failure are shown. To obtain these results, the kink angle that gave the maximum value of the energy release rate in the fiber was used, and this energy release rate was equated to  $\Gamma_f$ .

#### References

- K. M. Prewo, "Tension and Flexural Strength of Silicon Carbide Fibre-Reinforced Glass Ceramics," *J. Mater. Sci.*, **21**, 3590 (1986).
- J. Aveston, G. A. Cooper, and A. Kelly, "Single and Multiple Fracture"; pp. 15-26 in Conference Proceedings of the National Physical Laboratory: Properties of Fiber Composites. IPC Science and Technology Press, Surrey, England, 1971.
- D. B. Marshall and A. G. Evans, "Failure Mechanisms in Ceramic-Fiber/Ceramic-Matrix Composites," *J. Am. Ceram. Soc.*, **68** [5] 225-31 (1985).
- A. G. Evans, *Mater. Sci. Eng.*, **A107**, 227-41 (1989).
- B. Budiansky, J. W. Hutchinson, and A. G. Evans, *J. Mech. Phys. Solids*, **34**, 167 (1986).
- M. D. Thouless and A. G. Evans, *Acta Metall.*, **36**, 517 (1988).
- A. G. Evans, B. J. Dalgleish, M. Rühle, and M. D. Thouless, *Mater. Res. Soc. Proc.*, **78**, 259 (1987).
- G. Campbell, B. J. Dalgleish, M. Rühle, and A. G. Evans, "Whisker Toughening: A Comparison between  $\text{Al}_2\text{O}_3$  and  $\text{Si}_3\text{N}_4$  Toughened with SiC"; to be published in *J. Am. Ceram. Soc.*
- M. Y. He and J. W. Hutchinson, "Crack Deflection at an Interface between Dissimilar Elastic Materials"; to be published in *Int. J. Solids Struct.*
- M. Y. He and J. W. Hutchinson, "Kinking of a Crackout of an Interface," *J. Appl. Mech.*, **56**, 270-78 (1989).
- J. Dundurs, *Mathematical Theory of Dislocations*; p. 70. American Society of Mechanical Engineers, New York, 1969.
- P. G. Charalambides and A. G. Evans, "Debonding Properties of Residually Stressed Brittle-Matrix Composites," *J. Am. Ceram. Soc.*, **72** [5] 746-53 (1989).
- M. D. Thouless, H. C. Cao, and P. A. Mataga; to be published in *J. Mater. Sci.*
- A. G. Evans and J. W. Hutchinson, *Acta Metall.*, **37**, 909 (1989).
- M. D. Thouless, A. G. Evans, M. F. Ashby, and J. W. Hutchinson, *Acta Metall.*, **35**, 1333 (1987). □